forests

MDPI

Article

Transcriptome Analysis of Elm (*Ulmus pumila*) Fruit to Identify Phytonutrients Associated Genes and Pathways

Luoyan Zhang, Xuejie Zhang, Mengfei Li, Ning Wang, Xiaojian Qu and Shoujin Fan *

Key Lab of Plant Stress Research, College of Life Science, Shandong Normal University, Jinan 250014, China
* Correspondence: fansj@sdnu.edu.cn; Tel.: +86-0531-8618-0178

Received: 9 August 2019; Accepted: 26 August 2019; Published: 27 August 2019

Abstract: Plant fruit is an important source of natural active phytonutrients that are profitable for human health. Elm (*Ulmus pumila*) fruit is considered as natural plant food in China that is rich in nutrients. In the present study, high-throughput RNA sequencing was performed in *U. pumila* edible fruits and leaves and 11,386 unigenes were filtered as dysregulated genes in fruit samples, including 5231 up- and 6155 downregulated genes. Hundreds of pathways were predicted to participate in seed development and phytonutrient biosynthesis in *U. pumila* by GO, MapMan, and KEGG enrichment analysis, including "seed maturation", "glycine, serine, and threonine metabolism" and "phenylpropanoid biosynthesis". ABA-mediated glucose response-related ethylene-activated signaling pathway (e.g., ABI4) were supposed to associate with elm fruit development; unsaturated fatty acids pathway (e.g., ACX2 and SAD) were predicted to participate in determination of fatty acid composition in elm fruit; flavonoid and coumarins biosynthesis (e.g., CYP98A3 and CCoAOMT1) were demonstrated to correlate with the bioactivity of elm fruits in human cancer and inflammation resistance. To provide more information about fruit developmental status, the qRT-PCR analysis for key genes of "phenylpropanoid biosynthesis" and "alpha-Linolenic acid metabolism" were conducted in samples of young fruits, ripe fruit, old fruit, and leaves. Two biosynthetic pathways for unsaturated fatty acid and Jasmonic acid (JA) were deduced to be involved in fruit development in *U. pumila* and the phenylpropanoid glycoside, syringin, was speculated to accumulate in the early development stages of elm fruit. Our transcriptome data supports molecular clues for seed development and biologically active substances in elm fruits.

Keywords: *Ulmus pumila*; transcriptome analysis; phytonutrients; seed development; phenylpropanoid biosynthesis

1. Introduction

Human diets are recommended to be rich in vegetables and fruits, which are beneficial to human health. The relationship between plant food intake and health has been the focus of many scientific studies to determine specific plant components that are active in conveying health benefits [1]. It is commonly accepted that plant fruit is an important source of natural active phytonutrients for human health, including amino acids, vitamins, terpenoids, flavonoids, alkaloids, phenolic compounds, and other metabolites, which lessen the risk of chronic diseases, such as metabolic syndrome, cardiovascular disease, obesity, and cancer [2–4]. Studies of dietary intervention have concluded that eating fruit helps maintain a healthy weight and reduces the risk of a wide range of cancers and cardiovascular disease [5–7].

The current work examines the fruit and leaves of elm (*Ulmus pumila*) using Illumina sequencing. This species belongs to the botanical classification of Ulmaceae and is a deciduous tree native to central

Asia and is widely located in Asia, America, and southern Europe [8]. The species is a natural herb and of great economical value for use in traditional medicine in Asia. Humans use the stem and root parts of *U. pumila* for the treatment of various ailments such as edema, mastitis, gastric cancer, and inflammation in the traditional system of medicine [9,10]. Not surprisingly, a number of bioactive natural products have been identified from extracts of *U. pumila* [10–14].

The elm fruit is considered a plant food by the Chinese. The fruit contains about 3.3–4.5 g of proteins, 8.0–10.0 g of carbohydrate, and 1.0–1.5 g of dietary fiber per 100 g of fresh weight (FW), respectively [15–17]. It is also rich in vitamins (vitamin B1, vitamin B6, nicotinic acid, and ascorbic acid) and some minerals (calcium, potassium, magnesium, copper, iron) [15–17]. The elm fruit is considered useful for curing abscesses, infection, edema, cancer, and is of benefit for tonifying the spleen, treating insomnia, reducing blood glucose concentration, decreasing cholesterol and improving children's growth and development [15–17].

Although chemical, medical, and physiological evidence has been published for elm fruit, the molecular mechanisms of its phytonutrients remain partly unknown. Transcriptome sequencing is an effective method for genome-wide detection of potential participants of complex traits [18–27]. Dozens of studies in the field of fruit development and nutrition have implemented sequencing technologies [28–30]. In view of these facts, the work presented here was performed to uncover the key phytonutrient-associated genes and their regulators in elm fruit.

2. Materials and Methods

2.1. Plant Materials and RNA Extraction

Fruit and leaves of *U. pumila* were collected from the same tree in the specimen garden of the Shandong Normal University, Jinan, China, in March 2019. The elm fruits were classified by days after flowering (DAF) with different length and colors: young fruit, 20 DAF, 8–10 mm in length, and dark green color (fruit stage 1); young fruit, 30 DAF, 10–13 mm in length, and green color (fruit stage 2); ripe fruit, 40 DAF, 14–15 mm in length, and green color (fruit stage 3); and old fruit, 50 DAF, 14–15 mm in length, and yellow color (fruit stage 4). The fruits with 14–15 mm in length and green color (fruit stage 3) were identified as edible and were chosen for transcriptome analysis (Figure 1A,B). The selected fruits and leaves were collected and immediately frozen in liquid nitrogen and then stored at −80 °C until use. Three replicates of RNA extraction and transcriptome sequencing were performed for fruits and leaves. For each replicate, a total of 1 g of plant material was grinded in liquid nitrogen and TRIzol Reagent (Invitrogen, Carlsbad, CA, USA) was used for total RNA extraction according to the manufacturer's procedures. RNA Nano 6000 Assay Kit of the Agilent Bioanalyzer 2100 system (Agilent Technologies, Santa Clara, CA, USA) and a NanoDrop 2000 spectrophotometer (Thermo Scientific, Wilmington, NC, USA) were used for RNA quality assessment.

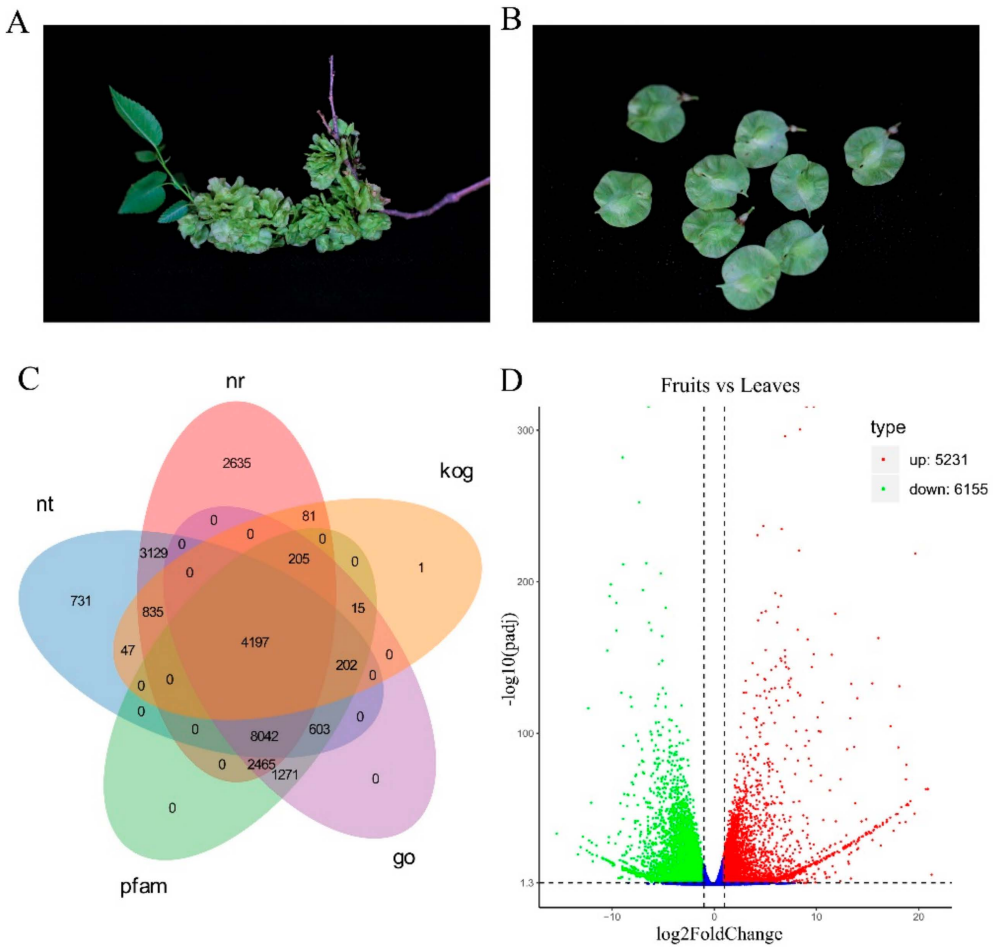

Figure 1. (**A**) The morphology of elm (*Ulmus pumila*) fruits and leaves. (**B**) The morphology of *U. pumila* fruits. (**C**) Venn diagram of functional annotations of unigenes in nt (NCBI nonredundant protein sequences), nr (NCBI nonredundant protein sequences), kog (Clusters of Orthologous Groups of proteins), go (Gene Ontology), and pfam (Protein family) databases. (**D**) Expression patterns of differentially expressed genes (DEGs) identified between fruits and leaves. Red and green dots represent DEGs, grey dots indicate genes that were not differentially expressed. In total, 11,386 unigenes were revealed to be differentially expressed (padj < 0.05) in fruit compared with control samples, with 5231 being upregulated and 6155 downregulated.

2.2. Library Construction and De Novo Assembly

NEBNext® UltraTM RNA Library Prep Kit for Illumina® (NEB, Beverly, MA, USA) were used to produce the RNA sequencing libraries. The mRNA purified by the poly-T oligo-attached magnetic beads and the synthesized cDNA (150–200 bp) were filtered by the AMPure XP system (Beckman Coulter, Beverly, MA, USA). After enriching and screening by PCR amplification, the products were sequenced by Illumina HiSeq × platform (Illumina, San Diego, CA, USA). Novogene Co., LTD were selected to perform cDNA library generation and PE150 sequencing. The clean reads were filtered by three steps: removing adapter, deleting poly-N reads and omitting low-quality reads. The Trinity software were used for de novo assembly [31]. The assembled sequences were annotated to public databases (NR, Pfam, KOG, KEGG, and Gene Ontology) by BLAST searches with an *E*-value cutoff of 1×10^{-5}. All sequencing data generated by this study have been submitted to the NCBI Sequence Read Archive (SRA) database [32], with accession: PRJNA545392.

2.3. Calculation of Genes' Expression and Enrichment Analyses in U. pumila

Six independent transcripts libraries were obtained for *U. pumila* by a PE150 sequencing. RSEM [33] were used to evaluate the gene expression levels. After the aligning the clean reads to the de novo assembled transcriptome, the fragment per kilobase of exon model per million mapped reads (FPKM) method [34] was selected to calculate genes' expression. The FPKM values between ripe fruit and leaf samples of all unigenes were compared by a threshold of |log2(foldchange)| > 1 and adjusted *p*-value < 0.05.

The unigenes of *U. pumila* were assigned to *A. thaliana* gene IDs by BLASTing the genome of *A. thaliana* with a cutoff of 1×10^{-5}. The topGO package of R and MapMan (version 3.5.1 R2) [35] were chosen for GO enrichment analysis and metabolic pathways enrichment for the differentially expressed genes (DEGs) in *U. pumila* fruit samples. The KEGG pathway enrichment analysis was performed by the software KOBAS [36].

2.4. qRT-PCR Analysis

The gene expression of four upregulated unigenes of "phenylpropanoid biosynthesis" pathway and four downregulated genes of "photosynthesis" pathway calculated by RNA-seq in ripe fruit and leave samples was validated by the qRT-PCR verification. Expression of eight key genes of "phenylpropanoid biosynthesis" (ko00940) and thirteen genes of "alpha-Linolenic acid metabolism" pathways (ko00592) were tested in samples of young fruits, ripe fruit, old fruit, and leaves by qRT-PCR analysis. The purified RNA samples were treated with DNaseI and converted to cDNA using the PrimeScript RT Reagent Kit with gDNA Eraser (Takara, Dalian, China). The ortholog of the *A. thaliana* member of Actin gene family ACT7 in *U. pumila* was used to normalize the amount of template cDNA. Premier 5.0 software was used to design gene-specific qRT-PCR primers (20–23 bp) (Table S5). qPCR analyses were performed on the ABI7500 Real-Time PCR System (ABI, USA) by using SYBR Green qPCR Master Mix (DBI, Germany). Each analysis was performed in triplicate and relative gene expression was quantified using the $2^{-(\Delta\Delta Ct)}$ method.

3. Results

3.1. Transcriptome Profiling of U. pumila

By sequencing with the Illumina HiSeq × platform, a total of 51,869,958, 54,374,336, 63,237,860, 66,499,546, 64,015,920, and 53,666,908 pair-end reads were acquired from three leaf and three fruit samples of *U. pumila*, respectively (Table 1). De novo transcriptome assembly yielded 35,416 unigenes, the average length of which was 1460 nt and N50 of 2251. Generally, 80.26% of the reads were mapped to the genome referenced for six samples of leaf and fruit (Table 1).

Table 1. Summary of mapping transcriptome reads to reference sequence in elm (*Ulmus pumila*).

Sample Name	Sample Description	Total Reads	Total Mapped	Ratio of Mapped Reads
Up_F_1	Fruits replication 1	51,869,958	41,402,822	79.82%
Up_F_2	Fruits replication 2	54,374,336	44,276,232	81.43%
Up_F_3	Fruits replication 3	63,237,860	51,316,902	81.15%
Up_L_1	Leaves replication 1	66,499,546	53,135,314	79.90%
Up_L_2	Leaves replication 2	64,015,920	50,704,484	79.21%
Up_L_3	Leaves replication 3	53,666,908	42,942,126	80.02%

3.2. Functional Annotations of Unigenes in U. pumila

BLASTX was used to perform similarity searches to annotate unigenes against various databases. All 35,416 (100%) unigenes were annotated in at least one database. A total of 21,589 (60.95%), 17,786 (50.22%), and 17,000 (48%) unigenes resembled the sequences in databases of NR, NT, and PFAM with an *E*-value threshold of 1×10^{-5} (Figure 1C). A total of 17,000 (48%) unigenes were annotated by

Blast2GO v2.5 in GO database with an *E*-value cutoff of 1×10^{-6}. A total of 21,255 unigenes of *U. pumila* were assigned to *A. thaliana* gene IDs for GO annotation mapping by BLASTX with an *E*-value cutoff of 1×10^{-5} and were used for MapMan analysis.

3.3. Differentially Expressed Genes (DEGs) Calculation in U. pumila

The relative expressional level of related genes in *U. pumila* fruits or leaves was evaluated by the FPKM values, which was computed following the uniquely mapped reads. The FPKM value for different genes ranged from 0.31 to 27,173.72, with a mean value of 30.28 detected in six samples. 5231 unigenes were filtered as upregulated and 6155 calculated as downregulated genes in fruit samples with the cutoff of |log2(foldchange)| > 1 and padj < 0.05 by comparative analysis (Figure 1D, Table S1). The 30 up- and downregulated genes are shown in Table 2. The lipids and proteins accumulation related protein oleosin 2 (Cluster-6074.11735, L_2fc = 9.880) and seed storage protein CRUCIFERINA (Cluster-6074.12126, L_2fc = 13.102) were identified as upregulated; the lipid-transfer protein (Cluster-6074.1319, L_2fc = −8.832) and pathogenesis-related thaumatin superfamily protein (Cluster-6074.23644, L_2fc = −7.223) were verified as the top downregulated genes (Table 2).

Table 2. The top 30 up- and downregulated genes.

Gene ID	L_2fc	Padj	Arabidopsis ID	Gene Description
Upregulated				
Cluster-6074.11735	9.880	0.00	AT5G40420	oleosin 2
Cluster-6074.11841	9.147	0.00		
Cluster-6074.12126	13.102	0.00	AT2G25890	
Cluster-6074.12191	18.879	0.00	AT5G44120	CRUCIFERINA
Cluster-6074.12375	13.383	0.00		
Cluster-6074.13108	18.27	0.00	AT1G03890	
Cluster-6074.12362	8.535	3.45×10^{-301}	AT1G62710	beta vacuolar processing enzyme
Cluster-6074.13152	7.047	9.73×10^{-297}	AT5G12380	annexin 8
Cluster-6074.12791	14.590	6.74×10^{-295}	AT4G25140	oleosin 1
Cluster-6074.12340	4.909	1.58×10^{-237}	AT5G49360	beta-xylosidase 1
Cluster-6074.11747	6.724	1.65×10^{-235}	AT5G12380	annexin 8
Cluster-6074.10421	4.358	2.17×10^{-231}	AT1G21410	
Cluster-6074.12488	8.434	2.01×10^{-221}	AT4G37370	cytochrome P450, family 81, subfamily D, polypeptide 8
Cluster-6074.12147	19.796	1.96×10^{-219}	AT1G03890	
Cluster-6074.13683	6.109	4.23×10^{-193}	AT1G04560	
Downregulated				
Cluster-6074.9536	−6.306	0.00		
Cluster-6074.1319	−8.832	8.48×10^{-283}	AT2G45180	
Cluster-6074.23644	−7.223	2.72×10^{-253}	AT1G20030	
Cluster-6074.18869	−6.508	6.11×10^{-213}	AT5G20740	
Cluster-6074.1201	−8.801	2.92×10^{-212}	AT4G11650	osmotin 34
Cluster-6074.20011	−5.099	3.94×10^{-206}	AT2G22540	short vegetative phase
Cluster-6074.25984	−9.979	6.56×10^{-199}		
Cluster-6074.18265	−6.868	2.59×10^{-195}	AT5G35630	glutamine synthetase 2
Cluster-6074.1293	−10.101	4.36×10^{-191}		
Cluster-6074.22654	−9.467	9.42×10^{-187}	AT5G59190	
Cluster-6074.1730	−4.625	1.19×10^{-183}	AT5G22430	
Cluster-6074.24974	−6.239	1.35×10^{-173}	AT5G67150	
Cluster-6074.16553	−6.034	9.25×10^{-169}	AT3G54420	homolog of carrot EP3-3 chitinase
Cluster-6074.1245	−9.437	2.26×10^{-168}		
Cluster-6074.21282	−4.960	8.82×10^{-165}	AT4G15440	hydroperoxide lyase 1

Note: L_2fc = Log_2 fold change.

3.4. GO, MapMan, and KEGG Enrichment Result of DEGs in U. pumila

To uncover the nutrient component-associated pathways in *U. pumila* fruit, the DEGs were described with GO databases. In total, 167 biological process (BP) terms were enriched with the cutoff of p-value < 0.05 by the 5231 upregulated unigenes, including "translation" (GO:0006412), "seed maturation" (GO:0010431), and "response to cadmium ion" (GO:0046686) (Table S2). A total of 173 BP terms were calculated to be enriched for the 6155 downregulated genes, such as "defense response" (GO:0006952), "photosynthesis" (GO:0015979), and "signal transduction" (GO:0007165) (Table S2).

As a result of the large numbers and the complex branch structure of GO categories, REVIGO was selected to uncover typical subgroups of the terms by employing a simple clustering algorithm, which is based on semantic similarity measures. The biological processes enriched by upregulated genes were pooled into eight groups (Figure 2A), 43 terms were summarized to the "translation" subset, including the BP terms "DNA demethylation" (GO:0080111), "biosynthetic process" (GO:0009058), and "unsaturated fatty acid biosynthetic process" (GO:0006636); 17 terms were classified to the "lipid storage" group; and 13 terms were assigned to the "seed maturation" group. In total, 3055 and 2960 homologs in *Arabidopsis* were assigned to up- and downregulated unigenes, respectively. A total of 1029 pathways were mapped by MapMan for these genes, of which, 117 pathways were filtered to be enriched by the dysregulated genes with the cutoff p-value < 0.05 (Table S3). The metabolism result of MapMan analysis is shown in Figure 2B.

The KEGG pathways enriched by upregulated unigenes are shown in Table S4 and the top 20 are represented in Figure S1A. The KEGG pathway "Ribosome" (ko03010) was enriched by 127 upregulated unigenes with rich_factor = 0.51, "Glycine, serine and threonine metabolism" (ko00052) was annotated for 29 overexpressed genes, and 49 upregulated genes were annotated in the KEGG pathway "Phenylpropanoid biosynthesis" (ko00940) (Figure S1A). The nutrition-related KEGG pathways enriched by upregulated genes are classified in Table 3. The "Amino acid" group included "Cysteine and methionine metabolism" (enriched with 29 upregulated genes), "Alanine, aspartate and glutamate metabolism" (enriched with 17 upregulated genes) and "Arginine biosynthesis" (enriched with 13 upregulated genes). A total of six fatty acid-related pathways are represented in Table 3, including "Fatty acid biosynthesis" (including 25 upregulated genes), "Biosynthesis of unsaturated fatty acids" (including nine upregulated genes) and "Glycerophospholipid metabolism" (including 24 upregulated genes). A total of 11 and seven unigenes were related to "Diterpenoid biosynthesis" and "Zeatin biosynthesis" pathways, respectively, and five unigenes related to "Vitamin B6 metabolism" pathway were upregulated in the fruit samples (Table 3, Table S4).

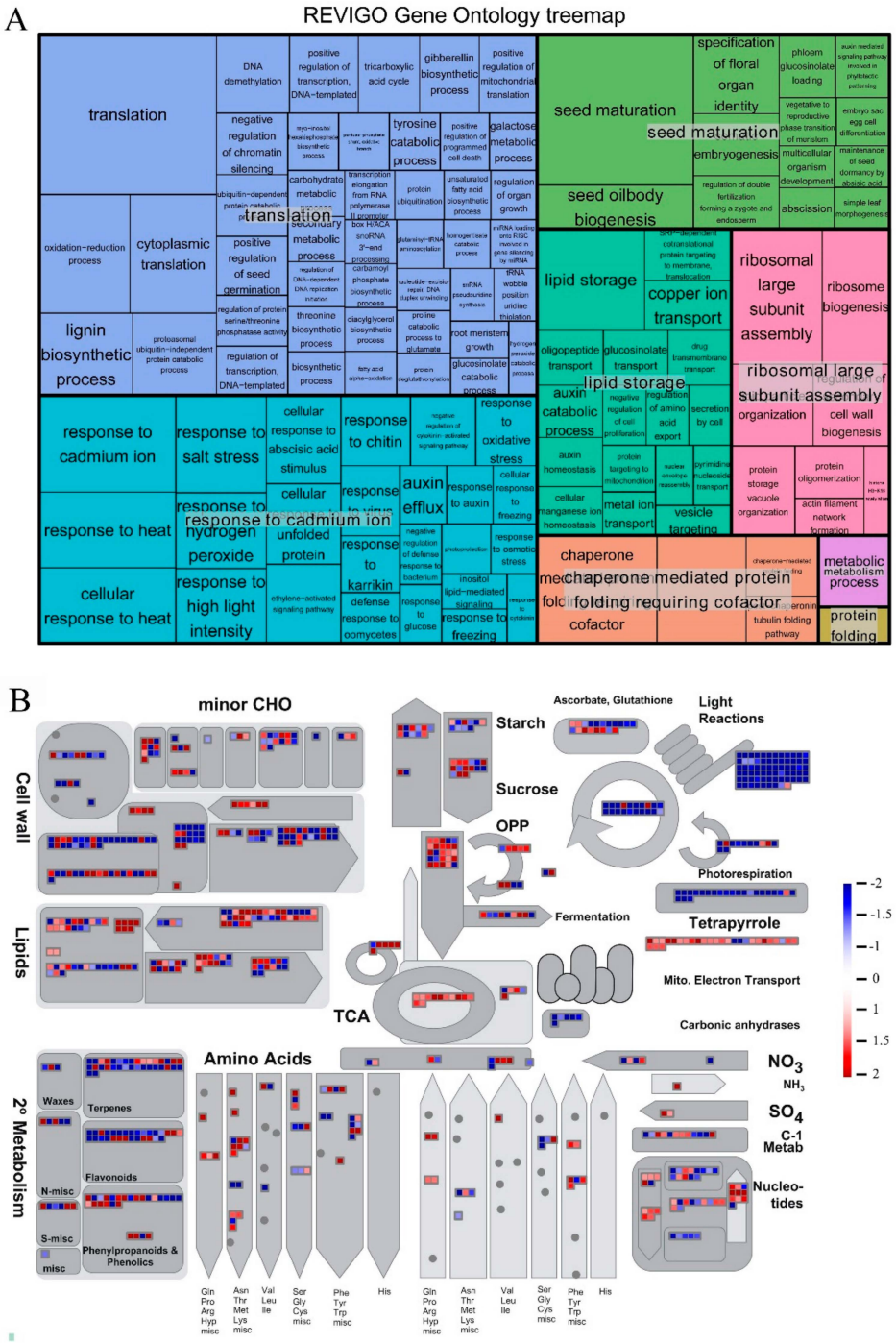

Figure 2. (**A**) REVIGO analysis for genes upregulated in *U. pumila* fruits. The representatives are classified into "superclusters" of loosely related terms, presented by different colors. The *p* value of the GO term is reflected by size of the rectangles which was calculated by TopGO. In this study, the biological processes enriched by upregulated genes were integrated into eight groups, 43 terms were summarized to the "translation" subset, 17 terms were classified to the "lipid storage" group, and 13 terms were assigned to the "seed maturation" group. (**B**) Differently expressed genes (DEGs) viewed globally, which are involved in diverse metabolic pathways. DEGs were chosen for the metabolic pathway analysis using the MapMan software (3.5.1 R2). Different colors of boxes indicate the Log_2 of the expression ratio of DEGs genes. In total, 3055 and 2960 homologs were assigned in *Arabidopsis* for the dysregulated unigenes, respectively. In total, 1029 pathways were mapped for these genes by MapMan, of which, 117 pathways were filtered to be enriched by the dysregulated genes with the cutoff *p*-value < 0.05 in ripe fruit.

Table 3. The nutrition-related KEGG pathways enriched by upregulated genes.

Item	Pathway	Annotated Gene Number	Enriched Gene Number
Amino acid	Glycine, serine and threonine metabolism	66	29
	Alanine, aspartate and glutamate metabolism	46	17
	Arginine biosynthesis	36	13
	Tyrosine metabolism	52	17
	Cysteine and methionine metabolism	99	29
	Cyanoamino acid metabolism	56	16
	Beta-Alanine metabolism	44	12
	Valine, leucine and isoleucine degradation	48	13
Fatty acid	Glycosphingolipid biosynthesis-globo series	10	4
	Fatty acid biosynthesis	65	25
	Selenocompound metabolism	22	7
	Biosynthesis of unsaturated fatty acids	31	9
	Glycerophospholipid metabolism	86	24
	Glycerolipid metabolism	72	19
Natural compounds	Diterpenoid biosynthesis	23	11
	Zeatin biosynthesis	18	7
	Phenylpropanoid biosynthesis	147	49
	Isoquinoline alkaloid biosynthesis	31	8
Vitamin	Biotin metabolism	19	7
	Vitamin B6 metabolism	14	5
	Ascorbate and aldarate metabolism	60	17

3.5. Real-Time Quantitative PCR Validation

To validate the RNA-Seq results in fruits of *U. pumila*, another strategy was chosen for the dysregulated unigenes. Four over- and four underregulated unigenes were selected for verification by real-time quantitative PCR (qRT-PCR) with the identical RNA samples that have been used for RNA-Seq. Primers were designed to span exon–exon junctions (Table S5). The expression trends of most test genes were similar between the RNA-Seq and qRT-PCR methods (Figure 3). For example, the homolog of SAD SSI2, Cluster-6074.5104, which was detected by RNA-Seq as an overexpressed unigene in the ripe fruit samples (L_2fc = 2.660), was also detected as significantly upregulated by qRT-PCR (Figure 3).

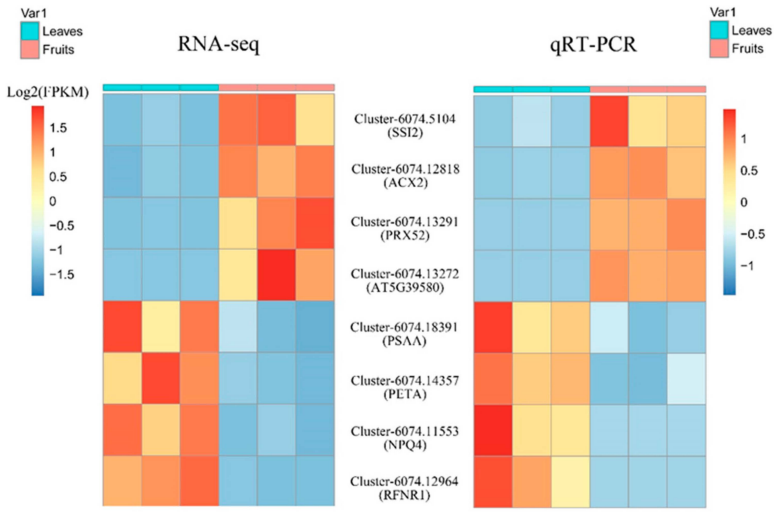

Figure 3. Validation of RNA-Seq results by qRT-PCR for eight *U. pumila* dysregulated genes. The expression of selected DEGs in fruits and leaves are shown. A red color indicates high expression for the gene in the fruit samples. Log_2(FPKM) means Log_2() value of FPKM for unigenes.

3.6. qRT-PCR Analysis for Phytonutrient-Associated Genes in Different Stages of Fruit Development

Information on the major gene expression variations that occur during fruit development has been predicted for edible ripe fruit (fruit stage 3); however, transcriptome analysis is limited to only

the matured stage. To provide more information about other fruit developmental stages, the qRT-PCR analysis for key genes in two phytonutrient-associated pathways were conducted in samples of young fruits (fruit stage 1–2), ripe fruit (fruit stage 3), old fruit (fruit stage 4), and leaves. In total, eight unigenes of lignin/Coniferin/Syringin metabolism in the "phenylpropanoid biosynthesis" (ko00940) pathway and 13 genes of the "alpha-Linolenic acid metabolism" (ko00592) pathway were selected for qRT-PCR analysis (Table S5).

Most of the unigenes upregulated in the "phenylpropanoid biosynthesis" pathway screened by RNA_seq were discovered to be overexpressed in the ripe fruit stage and all other fruit development stages by qRT-PCR (Figure 4A,B), including O-methyltransferase 1 (COMT) Cluster-6074.22341 (L_2fc = 2.515 in fruit stage 3/L_2fc = 1.837 in four fruit stages), cinnamoyl coa reductase 1 (CCR) Cluster-6074.9370 (L_2fc = 2.412/L_2fc = 1.308), GroES-like zinc-binding alcohol dehydrogenase family protein (CAD) Cluster-6074.16801 (L_2fc = 2.182/L_2fc = 1.013) and peroxidase superfamily protein (peroxidase) Cluster-6074.12541 (L_2fc = 15.679/L_2fc = 19.146). In total, nine of 13 unigenes in "alpha-Linolenic acid metabolism" pathway were uncovered as overexpressed in the ripe fruit and all other fruit stages compared with leaf (Figure S2A,B), including secretory phospholipase A2 (TGL4) Cluster-6074.14136 (L_2fc = 1.705/L_2fc = 1.481), lipoxygenase (LOX2S) Cluster-6074.3481 (L_2fc = 3.304/L_2fc = 3.319), acetyl-CoA acyltransferase (ACAA1) Cluster-6074.12598 (L_2fc = 7.907/L_2fc = 9.560), and enoyl-CoA hydratase/3-hydroxyacyl-CoA dehydrogenase (MFP2) Cluster-6074.13989 (L_2fc = 4.702/L_2fc = 4.534).

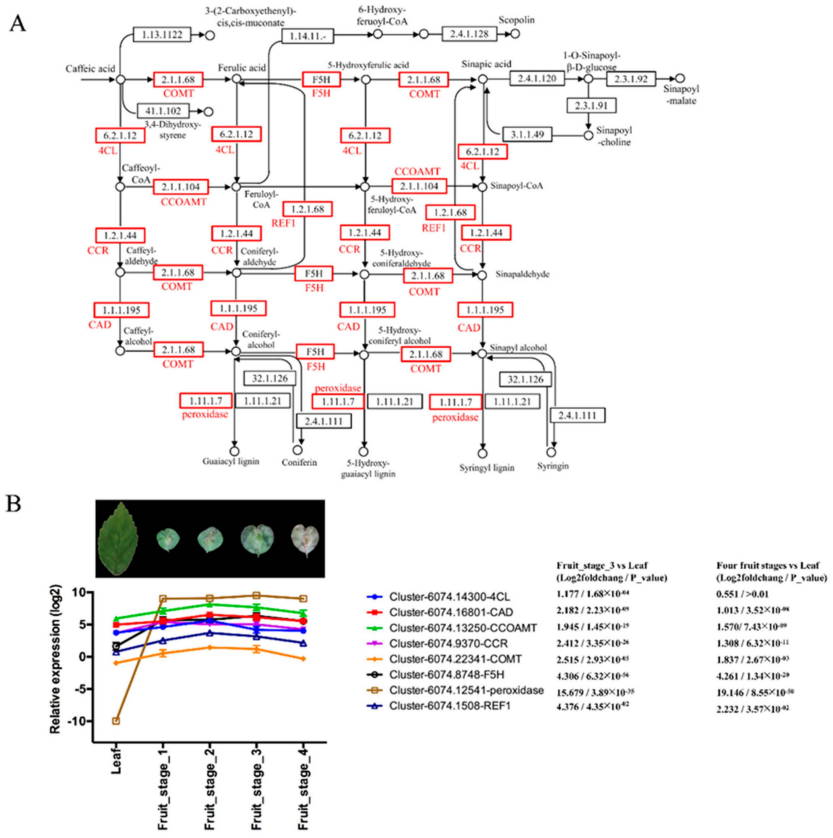

Figure 4. (**A**) The upregulated unigenes were mapped to lignin/Coniferin/Syringin metabolism in "phenylpropanoid biosynthesis" (ko00940) based on the KEGG database. The significantly upregulated genes in ko00940 are labeled with a red border. (**B**) Gene expression patterns of eight key genes were obtained by qRT-PCR analysis in young fruits (fruit stage 1–2), ripe fruit (fruit stage 3), old fruit (fruit stage 4), and leaves. The Log_2() fold change and *p*-value were listed for dysregulated unigenes in fruit stage 3 and four fruit stages compared with that of leaf.

4. Discussion

Plant fruits are an important source of naturally active phytonutrients which reduce the risk of cardiovascular disease, metabolic syndrome, and cancer [3,37–40]. *U. pumila* is used as traditional medicine and its fruit is considered a natural plant food in China rich in nutritional substances (proteins, dietary fiber, vitamins, and minerals) [15,41–43]. Although chemical, medical, and physiological evidence has been published for elm roots, leaves, and fruits, the molecular and genetic mechanism of its phytonutrient-associated metabolic processes remain unknown. Therefore, we attempted to uncover the key genes and pathways of elm fruit. RNA-Seq has been used to accurately monitor gene expression in hundreds of fruiting plants, such as sweet orange (*Citrus sinensis*) [44], mango (*Mangifera indica*) [28], *Cucumis melo* [45], and *Idesia polycarpa* [46], to track gene expression trends during fruit development. The synchronous dysregulation of key regulators in pathways verified by RNA-Seq and/or qRT-PCR analyses is valuable for understanding transcriptomic dynamics during elm fruit development. In this study, 11,386 unigenes were discovered to be differentially expressed in *U. pumila* fruits and leaves by RNA-seq, including 5231 up- and 6155 downregulated genes. Our transcriptome analysis contributes to understanding the molecular mechanisms for seed development and biologically active substances in *U. pumila* fruits.

Plant fruits develop primarily from the ovary following fertilization and seed development [47,48]. In this study, the processes "seed maturation" (GO:0010431), "embryo development ending in seed dormancy" (GO:0009793), and "seed oilbody biogenesis" (GO:0010344) were enriched by 50, 184, and six upregulated genes, respectively.

Several plant hormones are reported to control the regulation of fruit development and ripening, such as the gaseous hormone ethylene, abscisic acid (ABA), and gibberellin [49–51]. In this study, 59 upregulated genes were annotated in the "abscisic acid-activated signaling pathway" (GO:0009738), including *Arabidopsis* seed storage protein CRA1 (Cluster-6074.12833, L_2fc = 19.335) and seed maturation-associated ABA-responsive element binding protein AREB3 (Cluster-6074.15351, L_2fc = 1.998); 43 upregulated genes were annotated in "ethylene-activated signaling pathway" (GO:0009873), such as fatty acid accumulation during seed maturation related transcription factor WRI1 (Cluster-6074.11856, L_2fc = 10.875). ABA was found to promote the sensitivity to ethylene, enhancing the initiation and progression of ethylene-mediated fruit ripening processes [52]. In this study, ABA-mediated glucose response-related ethylene-activated signaling pathway member ABI4 (Cluster-6074.4471, L_2fc = 12.728), which participates in seed development in *Arabidopsis*, was significantly upregulated in elm fruit samples. Our transcriptome data provides evidence for the molecular mechanisms of elm fruit development.

Elm fruit contains significant amounts of vitamin B-complex, mainly B_1 (0.08–0.10 mg), B_2 (0.06–0.12 mg), and B_6 (1.20–1.50 mg) in 100 g FW [15–17]. In this study, five vitamin B_6 pathway-related unigenes were significantly upregulated in elm fruit compared with leaves, including pyridoxal phosphate synthase PDX1.2 (Cluster-6074.9816, L_2fc = 2.399), threonine synthase MTO2 (Cluster-6074.10873, L_2fc = 2.246), and pyridoxal reductase PLR1 (Cluster-6074.12916, L_2fc = 1.348). Vitamin B_6 with coenzymes performs various functions in the body. It is involved in amino acid/carbohydrate/lipid metabolism, cognitive development, gluconeogenesis and glycogenolysis, immune function, and hemoglobin formation [53–55]. In this study, 17 unigenes of the "Ascorbate and aldarate metabolism" (ko00053) pathway were upregulated in the fruit samples, such as GDP-l-galactose phosphorylase VTC2 (Cluster-6074.14130, L_2fc = 1.392) and L-Galactono-1,4-lactone dehydrogenase GLDH (Cluster-6074.25435, L_2fc = 5.210), which catalyzes the final step of ascorbate biosynthesis.

The lipid content of the elm fruit is restricted to the seeds and the defined fatty acids include 40–45% saturated fatty acids and 55–60% unsaturated fatty acids. In this study, nine unsaturated fatty acids pathway-associated unigenes were upregulated in elm fruit, including long chain fatty acid biosynthesis-related acyl-CoA oxidase ACX2 (Cluster-6074.12818, L_2fc = 2.499) and ACX4 (Cluster-6074.16191, L_2fc = 1.727), glyoxysomal fatty acid beta-oxidation pathway member stearoyl-acyl-carrier-protein desaturase (Cluster-6074.11259, L_2fc = 3.019), and peroxisomal

3-ketoacyl-CoA thiolase 3 (Cluster-6074.12598, L_2fc = 2.285). In plants, soluble stearoyl-acyl carrier protein (ACP) desaturase (SAD) was suggested to catalyze the conversion of stearoyl-ACP to oleoyol-ACP [56]. The ratio of saturated and unsaturated fatty acids is significantly influenced by the activity of SAD, and SAD is treated as a major determinant of fatty acid composition. The function of SAD in desirable fatty acid compositions has been identified in cacao (*Theobroma cacao*) [56], *Arabidopsis* [57], and peanut (*Arachis hypogaea*) [58]. In this study, the homolog of SAD SSI2 (Cluster-6074.5104, L_2fc = 2.660) was significantly upregulated in elm fruit, which indicated its function in determination of fatty acid composition.

Alpha-linolenic acid is an essential omega-3 fatty acid which is necessary for regular human growth and development. Alpha-linolenic acid protects against heart attacks, lowers blood pressure, reduces cholesterol, and reverses atherosclerosis. It is also used to treat multiple sclerosis, diabetes, ulcerative colitis, renal disease, and Crohn's disease [59]. In this study, proteins (secretory phospholipase A2, lipoxygenase) participating in metabolism of compounds alpha-Linolenic acid and (9Z,11E,15Z)-(13S)-Hydroperoxyoctadeca-9,11,15-trienoate and their coding genes were upregulated in the young and ripe elm fruits (Figure S2A,B). Downstream of the "alpha-Linolenic acid metabolism" pathway, genes for key enzymes (12-oxophytodienoic acid reductase, OPC-8:0 CoA ligase 1, acyl-CoA oxidase, enoyl-CoA hydratase and acetyl-CoA acyltransferase) which initiate jasmonic acid biosynthesis by shortening the beta-oxidative chain of its precursors were found to be synchronously overexpressed in all fruit stages (Figure S2A,B). Jasmonic acid (JA) and its derivatives are the best-studied signaling molecules derived from fatty acids. JA biosynthesis utilizes alpha-linolenic acid as a fatty acid substrate, which is released from the galactolipids of the chloroplast [60]. On the basis of gene regulation of alpha-linolenic acid and JA biosynthesis-related genes, unsaturated fatty acid biosynthesis and JA biosynthesis pathways were deduced to be involved in fruit development in *U. pumila*.

Phenylpropanoids (PPs) make up the largest portion of secondary metabolites produced by plants. As naturally occurring antioxidants, they have function in human tumors, inflammation, and cellular damage [61,62]. In this study, the "Phenylpropanoid biosynthesis" pathway was significantly enriched with 49 upregulated unigenes including many enzymes of this pathway, such as 4-coumarate-CoA ligase (Cluster-6074.14300, L_2fc = 1.077) and cinnamyl-alcohol dehydrogenase (Cluster-6074.20308, L_2fc = 4.604) (Figure S1B). Many phenolic compounds (flavonoids, coumarines, isoflavonoids, and lignans) derived from plants are secondary products of PP metabolism. Flavonoids have a favorable effect on cardiovascular disease, including anti-inflammatory functions [63,64], and coumarins derivatives have shown anticancer activity in various cancer cell lines. In this study, flavonoid and coumarins biosynthesis-associated oumarate 3-hydroxylase CYTOCHROME P450 (Cluster-6074.16505, L_2fc = 1.952), caffeoyl coenzyme A O-methyltransferase 1 (Cluster-6074.13250, L_2fc = 2.343), and lignin biosynthesis involved peroxidase 52 (Cluster-6074.13291, L_2fc = 9.155) were upregulated in the elm fruits. Our transcriptome data indicated the PPs might be associated with the bioactivity of elm fruits in human cancer and inflammation resistance.

Eleutheroside B (syringin) is a phenylpropanoid glycoside first isolated from *Acanthopanax senticosus* and has neuroprotective, tonic, adaptogenic, and immune-modulating properties. Syringin has a potent protection against LPS/D-GalN-induced fulminant hepatic failure, and it activates Nrf2 and inhibits the NF-κB signaling pathway to attenuate LPS-induced acute lung injury [62,63,65]. In this study, expression of genes encoding key enzymes (4-coumarate-CoA ligase, cinnamoyl-CoA reductase, and cinnamyl-alcohol dehydrogenase) which transform sinapic acid to intermediates of syringin (sinapoyl-CoA, sinapoyl aldehyde, and sinapyl alcohol) showed an increase from fruit stage 1 (young fruit) to fruit stage 3 (ripe fruit) and decreased in the old fruit stage, indicating syringin accumulation in the early fruit development stages.

5. Conclusions

Transcriptome analysis was performed for ripe *U. pumila* fruit. In total, 5231 unigenes were filtered as upregulated in edible fruit samples and 6155 were downregulated in *U. pumila*. Hundreds of

pathways were predicted to participate in seed development and phytonutrients biosynthesis in *U. pumila* by GO, MapMan, and KEGG enrichment analysis. The pathways "seed maturation", "glycine, serine, and threonine metabolism", and "phenylpropanoid biosynthesis" were found to be highly expressed in fruits. The ABA-mediated glucose response-related ethylene-activated signaling pathway (e.g., ABI4) was associated with elm fruit development; the unsaturated fatty acids pathway (e.g., ACX2 and SAD) was predicted to participate in determinant of fatty acid composition in elm fruit; flavonoid and coumarins biosynthesis (e.g., CYP98A3 and CCoAOMT1) were found to be related to the bioactivity of elm fruit in human cancer and inflammation resistance. To provide more information about other fruit developmental stages, qRT-PCR analysis for key genes of "phenylpropanoid biosynthesis" and "alpha-Linolenic acid metabolism" were conducted in samples of young fruits, ripe fruit, old fruit, and leaves. Two biosynthetic pathways for unsaturated fatty acid and JA were involved in fruit development in *U. pumila* and syringin is speculated to accumulate in the early development stages of elm fruit.

Data Archiving Statement

All genetic data have been submitted to the NCBI Sequence Read Archive (SRA) database (https://submit.ncbi.nlm.nih.gov/subs/sra), PRJNA545392 for *U. pumila*.

Supplementary Materials: The following are available online at http://www.mdpi.com/1999-4907/10/9/738/s1, Table S1. Information of unigenes dysregulated in *elm (Ulmus pumila)*. Table S2. GO enrichment analysis of genes differentially expressed in *U. pumila* fruits. Table S3. MapMan enrichment analysis of genes differentially expressed in *U. pumila* fruits. Table S4. KEGG enrichment analysis of genes differentially expressed in *U. pumila* fruits. Table S5. qRT -PCR primers. Figure S1. (A) Scatterplot of top 20 KEGG pathways enriched by upregulated unigenes. Rich factor represents the ratio of the number of differentially expressed genes (DEG)s and the number of all genes in the pathway. The KEGG pathway "Ribosome" (ko03010) was enriched by 127 upregulated unigenes, "Glycine, serine and threonine metabolism" (ko00052) were annotated by 29 over-expressed genes and 49 upregulated genes were annotated in the KEGG pathway "Phenylpropanoid biosynthesis" (ko00940). (B) "Phenylpropanoid biosynthesis" (ko00940) pathway enriched by the upregulated unigenes based on the KEGG database. The significantly upregulated genes in ko00940 were labeled with red bracket. Figure S2. (A) The upregulated unigenes were mapped to "alpha-Linolenic acid metabolism" pathways (ko00592) based on the KEGG database. The significantly upregulated genes in ko00592 were labeled with red bracket. (B) Gene expression patterns of nine upregulated key genes obtained by qRT-PCR analysis in young fruits (fruit stage 1–2), ripe fruit (fruit stage 3), old fruit (fruit stage 4), and leaves. The $Log_2()$ fold change and *p*-value were listed for dysregulated unigenes in fruit stage 3 and four fruit stages compared with that of leaf.

Author Contributions: Conceptualization, L.Z., X.Z., M.L. and S.F.; Data curation: L.Z., X.Z., M.L., N.W. and X.Q.; Funding acquisition, L.Z. and S.F.; Investigation, L.Z., M.L., N.W. and X.Q.; Methodology, L.Z.; Software, X.Z.; Supervision, S.F.; Writing—Original draft, L.Z., X.Z. and S.F.; Writing—Review & editing, S.F.

Funding: This work was supported by Natural Science Foundation of China (31800185, 31470298) and the Science and Technology Development Foundation of Shandong Province (2018LZGC038). A Project of Shandong Province Higher Educational Science and Technology Program (J18KA147).

Acknowledgments: This work was supported by Natural Science Foundation of China (31800185, 31470298) and the Science and Technology Development Foundation of Shandong Province (2018LZGC038). A Project of Shandong Province Higher Educational Science and Technology Program (J18KA147).

Conflicts of Interest: The authors declare no conflict of interest.

References

1. Kris-Etherton, P.M.; Hecker, K.D.; Bonanome, A.; Coval, S.M.; Binkoski, A.E.; Hilpert, K.F.; Griel, A.E.; Etherton, T.D. Bioactive compounds in foods: Their role in the prevention of cardiovascular disease and cancer. *Am. J. Med.* **2002**, *113*, 71–88. [CrossRef]
2. Lampe, J.W. Health effects of vegetables and fruit: Assessing mechanisms of action in human experimental studies. *Am. J. Clin. Nutr.* **1999**, *70*, 475s–490s. [CrossRef]
3. Neto, C.C. Cranberry and blueberry: Evidence for protective effects against cancer and vascular diseases. *Mol. Nutr. Food Res.* **2010**, *51*, 652–664. [CrossRef]
4. Fernie, A.R.; Schauer, N. Metabolomics-assisted breeding: A viable option for crop improvement? *Trends Genet.* **2009**, *25*, 39–48. [CrossRef] [PubMed]

5. Wang, Q.; Chen, Y.; Wang, X.; Gong, G.; Li, G.; Li, C. Consumption of fruit, but not vegetables, may reduce risk of gastric cancer: Results from a meta-analysis of cohort studies. *Eur. J. Cancer* **2014**, *50*, 1498–1509. [CrossRef]
6. Everitt, A.V.; Hilmer, S.N.; Brandmiller, J.C.; Jamieson, H.A.; Truswell, A.S.; Sharma, A.P.; Mason, R.S.; Morris, B.J.; Le, C.D. Dietary approaches that delay age-related diseases. *Clin. Interv. Aging* **2006**, *1*, 11–31. [CrossRef] [PubMed]
7. Bendinelli, B.; Masala, G.; Saieva, C.; Salvini, S.; Calonico, C.; Sacerdote, C.; Agnoli, C.; Grioni, S.; Frasca, G.; Mattiello, A. Fruit, vegetables, and olive oil and risk of coronary heart disease in Italian women: The EPICOR Study. *Am. J. Clin. Nutr.* **2011**, *94*, 287–288. [CrossRef]
8. Wiegrefe, S.J.; Sytsma, K.J.; Guries, R.P. Phylogeny of elms (Ulmus, Ulmaceae): Molecular evidence for a sectional classification. *Syst. Bot.* **1994**, *19*, 590–612. [CrossRef]
9. Ghosh, C.; Yang, S.H.; Hwang, S.G. Methanol extract of *Ulmus pumila*. L exerts potent anti-inflammatory effects in murine macrophages and mouse skin. *FASEB J.* **2013**, *27*, 1093.
10. Wang, D.; Xia, M.Y.; Cui, Z. New triterpenoids isolated from the root bark of *Ulmus pumila* L. *Chem. Pharm. Bull.* **2006**, *54*, 775–778. [CrossRef]
11. Feng, Z.T.; Deng, Y.Q.; Fan, H.; Sun, Q.J.; Sui, N.; Wang, B.S. Effects of NaCl stress on the growth and photosynthetic characteristics of *Ulmus pumila* L. seedlings in sand culture. *Photosynthetica* **2014**, *52*, 313–320. [CrossRef]
12. Mu, D.Y.; Zwiazek, J.J.; Li, Z.Q.; Zhang, W.Q. Genotypic variation in salt tolerance of *Ulmus pumila* plants obtained by shoot micropropagation. *Acta Physiol. Plant* **2016**, *38*, 188. [CrossRef]
13. Zhu, J.F.; Yang, X.Y.; Liu, Z.X.; Zhang, H.X. Identification and Target Prediction of MicroRNAs in *Ulmus pumila* L. Seedling Roots under Salt Stress by High-Throughput Sequencing. *Forests* **2016**, *7*, 318. [CrossRef]
14. Zhou, Z.H.; Shao, H.J.; Han, X.; Wang, K.J.; Gong, C.P.; Yang, X.B. The extraction efficiency enhancement of polyphenols from *Ulmus pumila* L. barks by trienzyme-assisted extraction. *Ind. Crop Prod.* **2017**, *97*, 401–408. [CrossRef]
15. Yu, S.L. Nutrition and health effects of elm fruits. *Food Nutr. China* **2009**, *9*, 60–62.
16. Li, Y.; Wang, Y.; Xue, H.; Pritchard, H.W.; Wang, X.F. Changes in the mitochondrial protein profile due to ROS eruption during ageing of elm (*Ulmus pumila* L.) seeds. *Plant Physiol. Biochem.* **2017**, *114*, 72–87. [CrossRef] [PubMed]
17. Wang, Y.; Li, Y.; Xue, H.; Pritchard, H.W.; Wang, X.F. Reactive oxygen species-provoked mitochondria-dependent cell death during ageing of elm (*Ulmus pumila* L.) seeds. *Plant J.* **2015**, *81*, 438–452. [CrossRef] [PubMed]
18. Yuan, F.; Lyu, M.J.A.; Leng, B.Y.; Zhu, X.G.; Wang, B.S. The transcriptome of NaCl-treated *Limonium bicolor* leaves reveals the genes controlling salt secretion of salt gland. *Plant Mol. Biol.* **2016**, *91*, 241–256. [CrossRef]
19. Zhang, H.; Zhang, Q.; Zhai, H.; Li, Y.; Wang, X.; Liu, Q.; He, S. Transcript profile analysis reveals important roles of jasmonic acid signalling pathway in the response of sweet potato to salt stress. *Sci. Rep. UK* **2017**, *7*, 40819. [CrossRef]
20. Yuan, F.; Lyu, M.J.A.; Leng, B.Y.; Zheng, G.Y.; Feng, Z.T.; Li, P.H.; Zhu, X.G.; Wang, B.S. Comparative transcriptome analysis of developmental stages of the *Limonium bicolor* leaf generates insights into salt gland differentiation. *Plant Cell Environ.* **2015**, *38*, 1637–1657. [CrossRef]
21. Xu, J.J.; Li, Y.Y.; Ma, X.L.; Ding, J.F.; Wang, K.; Wang, S.S.; Tian, Y.; Zhang, H.; Zhu, X.G. Whole transcriptome analysis using next-generation sequencing of model species *Setaria viridis* to support C-4 photosynthesis research. *Plant Mol. Biol.* **2013**, *83*, 77–87. [CrossRef] [PubMed]
22. Lin, J.; Li, J.P.; Yuan, F.; Yang, Z.; Wang, B.S.; Chen, M. Transcriptome profiling of genes involved in photosynthesis in *Elaeagnus angustifolia* L. under salt stress. *Photosynthetica* **2018**, *56*, 998–1009. [CrossRef]
23. Yang, S.; Li, L.; Zhang, J.L.; Geng, Y.; Guo, F.; Wang, J.G.; Meng, J.J.; Sui, N.; Wan, S.B.; Li, X.G. Transcriptome and Differential Expression Profiling Analysis of the Mechanism of Ca^{2+} Regulation in Peanut (*Arachis hypogaea*) Pod Development. *Front. Plant Sci.* **2017**, *8*, 1609. [CrossRef] [PubMed]
24. Yang, Z.; Wang, Y.; Wei, X.C.; Zhao, X.; Wang, B.S.; Sui, N. Transcription Profiles of Genes Related to Hormonal Regulations Under Salt Stress in Sweet Sorghum. *Plant Mol. Biol. Rep.* **2017**, *35*, 586–599. [CrossRef]
25. Du, M.F.; Ding, G.J.; Cai, Q.O. The Transcriptomic Responses of *Pinus massoniana* to Drought Stress. *Forests* **2018**, *9*, 326. [CrossRef]

26. Cai, Q.F.; Li, B.; Lin, F.R.; Huang, P.; Guo, W.Y.; Zheng, Y.Q. De Novo Sequencing and Assembly Analysis of Transcriptome in *Pinus bungeana* Zucc. ex Endl. *Forests* **2018**, *9*, 156. [CrossRef]
27. Zhao, D.Q.; Zhang, X.Y.; Fang, Z.W.; Wu, Y.Q.; Tao, J. Physiological and Transcriptomic Analysis of Tree Peony (Paeonia section Moutan DC.) in Response to Drought Stress. *Forests* **2019**, *10*, 135. [CrossRef]
28. Wu, H.X.; Jia, H.M.; Ma, X.W.; Wang, S.B.; Yao, Q.S.; Xu, W.T.; Zhou, Y.G.; Gao, Z.S.; Zhan, R.L. Transcriptome and proteomic analysis of mango (*Mangifera indica* Linn) fruits. *J. Proteom.* **2014**, *105*, 19–30. [CrossRef]
29. Munoz-Espinoza, C.; Di Genova, A.; Correa, J.; Silva, R.; Maass, A.; Gonzalez-Aguero, M.; Orellana, A.; Hinrichsen, P. Transcriptome profiling of grapevine seedless segregants during berry development reveals candidate genes associated with berry weight. *BMC Plant Biol.* **2016**, *16*, 104. [CrossRef]
30. Sweetman, C.; Wong, D.C.J.; Ford, C.M.; Drew, D.P. Transcriptome analysis at four developmental stages of grape berry (*Vitis vinifera* cv. Shiraz) provides insights into regulated and coordinated gene expression. *BMC Genom.* **2012**, *13*, 691. [CrossRef]
31. Grabherr, M.G.; Haas, B.J.; Moran, Y.; Levin, J.Z.; Thompson, D.A.; Ido, A.; Xian, A.; Lin, F.; Raktima, R.; Qiandong, Z. Full-length transcriptome assembly from RNA-Seq data without a reference genome. *Nat. Biotechnol.* **2011**, *29*, 644. [CrossRef] [PubMed]
32. NCBI Sequence Read Archive (SRA) Database. Available online: https://www.ncbi.nlm.nih.gov/sra (accessed on 27 August 2019).
33. Bo, L.; Dewey, C.N. RSEM: Accurate transcript quantification from RNA-Seq data with or without a reference genome. *BMC Bioinform.* **2011**, *12*, 323.
34. Haas, B.J.; Alexie, P.; Moran, Y.; Manfred, G.; Blood, P.D.; Joshua, B.; Matthew Brian, C.; David, E.; Bo, L.; Matthias, L. De novo transcript sequence reconstruction from RNA-seq using the Trinity platform for reference generation and analysis. *Nat. Protoc.* **2013**, *8*, 1494–1512. [CrossRef] [PubMed]
35. Thimm, O.; Blasing, O.; Gibon, Y.; Nagel, A.; Meyer, S.; Kruger, P.; Selbig, J.; Muller, L.A.; Rhee, S.Y.; Stitt, M. MAPMAN: A user-driven tool to display genomics data sets onto diagrams of metabolic pathways and other biological processes. *Plant J.* **2010**, *37*, 914–939. [CrossRef]
36. Chen, X.; Xizeng, M.; Jiaju, H.; Yang, D.; Jianmin, W.; Shan, D.; Lei, K.; Ge, G.; Chuan-Yun, L.; Liping, W. KOBAS 2.0: A web server for annotation and identification of enriched pathways and diseases. *Nucleic Acids Res.* **2011**, *39*, 316–322.
37. Latocha, P. The Nutritional and Health Benefits of Kiwiberry (*Actinidia arguta*)—A Review. *Plant Food Hum. Nutr.* **2017**, *72*, 325–334. [CrossRef]
38. Aune, D.; Giovannucci, E.; Boffetta, P.; Fadnes, L.T.; Keum, N.; Norat, T.; Greenwood, D.C.; Riboli, E.; Vatten, L.J.; Tonstad, S. Fruit and vegetable intake and the risk of cardiovascular disease, total cancer and all-cause mortality-a systematic review and dose-response meta-analysis of prospective studies. *Int. J. Epidemiol.* **2017**, *46*, 1029–1056. [CrossRef]
39. Block, G.; Patterson, B.; Subar, A. Fruit, vegetables, and cancer prevention: A review of the epidemiological evidence. *Nutr. Cancer* **1992**, *18*, 1–29. [CrossRef]
40. Steinmetz, K.A.; Potter, J.D. Vegetables, fruit, and cancer prevention: A review. *J. Am. Diet Assoc.* **1996**, *96*, 1027–1039. [CrossRef]
41. Dukic, M.; Dunisijevic-Bojovic, D.; Samuilov, S. The Influence of Cadmium and Lead on *Ulmus Pumila* L. Seed Germination and Early Seedling Growth. *Arch. Biol. Sci.* **2014**, *66*, 253–259. [CrossRef]
42. Ghosh, C.; Chung, H.Y.; Nandre, R.M.; Lee, J.H.; Jeond, T.I.; Kim, I.S.; Yang, S.H.; Hwang, S.G. An active extract of *Ulmus pumila* inhibits adipogenesis through regulation of cell cycle progression in 3T3-L1 cells. *Food Chem. Toxicol.* **2012**, *50*, 2009–2015. [CrossRef] [PubMed]
43. Qin, J.; Xi, W.M.; Rahmlow, A.; Kong, H.Y.; Zhang, Z.; Shangguan, Z.P. Effects of forest plantation types on leaf traits of *Ulmus pumila* and *Robinia pseudoacacia* on the Loess Plateau, China. *Ecol. Eng.* **2016**, *97*, 416–425. [CrossRef]
44. Yu, K.; Xu, Q.; Da, X.; Guo, F.; Ding, Y.; Deng, X. Transcriptome changes during fruit development and ripening of sweet orange (*Citrus sinensis*). *BMC Genom.* **2012**, *13*, 10. [CrossRef] [PubMed]
45. Zhang, H.; Wang, H.; Yi, H.; Zhai, W.; Wang, G.; Fu, Q. Transcriptome profiling of *Cucumis melo* fruit development and ripening. *Hortic. Res.* **2016**, *3*, 16014. [CrossRef] [PubMed]
46. Li, R.J.; Gao, X.; Li, L.M.; Liu, X.L.; Wang, Z.Y.; Lü, S.Y. *De novo* assembly and characterization of the fruit transcriptome of *Idesia polycarpa* reveals candidate genes for lipid biosynthesis. *Front. Plant Sci.* **2016**, *7*, 801. [CrossRef] [PubMed]

47. Barbosa, J.; Teixeira, P. Development of probiotic fruit juice powders by spray-drying: A review. *Food Rev. Int.* **2017**, *33*, 335–358. [CrossRef]
48. Seymour, G.B.; Ostergaard, L.; Chapman, N.H.; Knapp, S.; Martin, C. Fruit development and ripening. *Annu. Rev. Plant Biol.* **2013**, *64*, 219–241. [CrossRef]
49. Kumar, R.; Khurana, A.; Sharma, A.K. Role of plant hormones and their interplay in development and ripening of fleshy fruits. *J. Exp. Bot.* **2014**, *65*, 4561–4575. [CrossRef]
50. Zhu, Y.M.; Zheng, P.; Varanasi, V.; Shin, S.B.; Main, D.; Curry, E.; Mattheis, J.P. Multiple plant hormones and cell wall metabolism regulate apple fruit maturation patterns and texture attributes. *Tree Genet. Genomes* **2012**, *8*, 1389–1406. [CrossRef]
51. Xue, S.; Dong, M.; Liu, X.; Xu, S.; Pang, J.; Zhang, W.; Weng, Y.; Ren, H. Classification of fruit trichomes in cucumber and effects of plant hormones on type II fruit trichome development. *Planta* **2019**, *249*, 407–416. [CrossRef]
52. Jiang, Y.; Joyce, D.C.; Macnish, A.J. Effect of Abscisic Acid on Banana Fruit Ripening in Relation to the Role of Ethylene. *J. Plant Growth Regul.* **2000**, *19*, 106–111. [CrossRef] [PubMed]
53. Balk, E.M.; Raman, G.; Tatsioni, A.; Chung, M.; Lau, J.; Rosenberg, I.H. Vitamin B6, B12, and folic acid supplementation and cognitive function: A systematic review of randomized trials. *Arch. Intern. Med.* **2007**, *167*, 21–30. [CrossRef] [PubMed]
54. Mathers, J.C. Plant foods for human health: Research challenges. *Proc. Nutr. Soc.* **2006**, *65*, 198–203. [CrossRef] [PubMed]
55. Luthje, S.; Deswal, R.; Agrawal, G.K. Plant-based Foods: Seed, Nutrition and Human Health. *Proteomics* **2015**, *15*, 1638. [CrossRef] [PubMed]
56. Zhang, Y.; Maximova, S.N.; Guiltinan, M.J. Characterization of a stearoyl-acyl carrier protein desaturase gene family from chocolate tree, *Theobroma cacao* L. *Front. Plant Sci.* **2015**, *6*, 239. [CrossRef] [PubMed]
57. Bryant, F.M.; Munoz-Azcarate, O.; Kelly, A.A.; Beaudoin, F.; Kurup, S.; Eastmond, P.J. ACYL-ACYL CARRIER PROTEIN DESATURASE2 and 3 Are Responsible for Making Omega-7 Fatty Acids in the Arabidopsis Aleurone. *Plant Physiol.* **2016**, *172*, 154–162. [CrossRef]
58. Chi, X.; Yang, Q.; Pan, L.; Chen, M.; He, Y.; Yang, Z.; Yu, S. Isolation and characterization of fatty acid desaturase genes from peanut (*Arachis hypogaea* L.). *Plant Cell Rep.* **2011**, *30*, 1393–1404. [CrossRef]
59. Gerber, M. Omega-3 fatty acids and cancers: A systematic update review of epidemiological studies. *Br. J. Nutr.* **2012**, *107*, S228–S239. [CrossRef]
60. Weber, H. Fatty acid-derived signals in plants. *Trends Plant Sci.* **2002**, *7*, 217–224. [CrossRef]
61. Hemaiswarya, S.; Doble, M. Combination of phenylpropanoids with 5-fluorouracil as anti-cancer agents against human cervical cancer (HeLa) cell line. *Phytomedicine* **2013**, *20*, 151–158. [CrossRef]
62. Rochfort, S.; Parker, A.J.; Dunshea, F.R. Plant bioactives for ruminant health and productivity. *Phytochemistry* **2008**, *69*, 299–322. [CrossRef] [PubMed]
63. Le Marchand, L. Cancer preventive effects of flavonoids—A review. *Biomed. Pharmacother.* **2002**, *56*, 296–301. [CrossRef]
64. Romagnolo, D.F.; Selmin, O.I. Flavonoids and cancer prevention: A review of the evidence. *J. Nutr. Gerontol. Geriatr.* **2012**, *31*, 206–238. [CrossRef] [PubMed]
65. Krishnan, S.S.C.; Subramanian, I.P.; Subramanian, S.P. Isolation, characterization of syringin, phenylpropanoid glycoside from, *Musa paradisiaca*, tepal extract and evaluation of its antidiabetic effect in streptozotocin-induced diabetic rats. *Biomed. Prev. Nutr.* **2014**, *4*, 105–111. [CrossRef]